VI International Conference on Particle-based Methods – Fundamentals and Applications
PARTICLES 2019
E. Oñate, M. Bischoff, D.R.J. Owen, P. Wriggers & T. Zohdi (Eds)

PARAMETER IDENTIFICATION FOR DISCRETE ELEMENT SIMULATION OF VERTICAL FILLING: IN-SITU BULK CALIBRATION FOR REALISTIC GRANULAR FOODS

Stefan Kirsch[1,2]

[1] Technische Universität Dresden

[2] Bosch Packaging Technology B.V.
Postbus 16, 6000AA Weert, The Netherlands
stefan.kirsch2@bosch.com

Key words: Vertical filling, Granular foods, Tubular bagger, DEM, CFD, Air Resistance

Abstract. Vertical filling of granular media is influenced by resistance of the surrounding medium, especially in the case of a dilute process with relatively large distances between particles and relatively low particle densities. Discrete Element simulations were carried out to calibrate models of such a filling process for two granular food goods. The aim was to perform bulk calibration in-situ, meaning in the process of interest itself, rather than a second setup. To account for the air drag but keep computational cost practical, the computationally cheap free fall was modeled with the Schiller-Naumann correlation for drag force. The predictions where compared to simulations without fluid influence. The results show that the predictive quality of the models was increased with the simple drag model. It is shown that with the expanded model, calibration can be performed in the filling process itself, which might be useful especially for industry application.

1 INTRODUCTION

Vertical filling is a staple in the industrial packaging of granular foods, such as candy, cereal, nuts and pasta. The most common example is the vertical form, fill and sealing process (VFFS), which is capable of producing and filling over a hundred bags per minute. The process is shown schematically in figure 1a.

After a dosing unit has filled the collection bucket with a defined amount of good, the particles are released and fall through the forming tube. The latter is surrounded by a downwards moving film tube. As the sealing jaws close, they seal both the bottom of the current bag as well as the top of the last bag. The bag production rate is often limited by the falling behavior of the bulk good. This is due to the fact that in each cycle, all particles must entirely fall past the sealing jaws which are only open for a limited amount of time between sealing events. The maximum time allowed for filling t_{fill}, must thus be longer than the time between the first and the last particle to leave the tube at the bottom. The relationship between the events of each bag production cycle are shown in

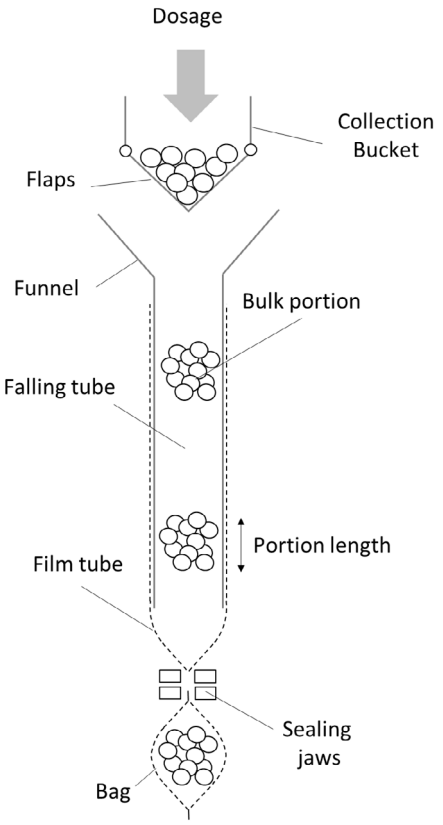

(a) Schematic filling in a vertical tubular bagger (VFFS). Adapted from[1].

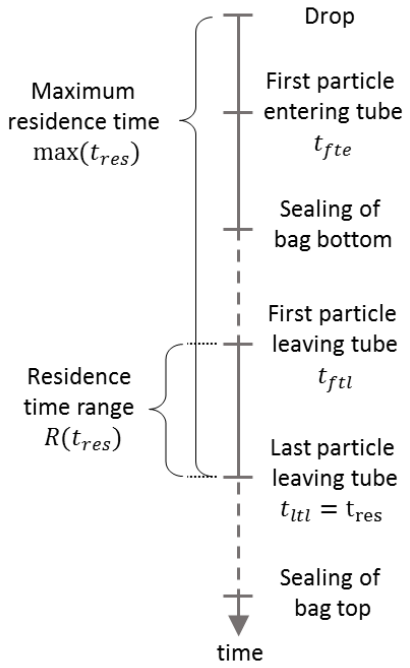

(b) Events in each cycle of bag filling. The dashed lines represent indicate variable buffer times which are necessary to accomodate random variation. From [2].

Figure 1: Overview of the vertical filling process.

figure 1b. The time allowed for filling t_{fill} must be longer than the range of the particle residence time $R(t_{res})$, i.e. the residence time of the last particle to leave the tube t_{ltl} minus the residence time of the first particle to leave the tube t_{ftl}.

$$t_{fill} \overset{!}{>} R(tres) = t_{ltl} - t_{fte} \tag{1}$$

To accommodate random variation in the falling behavior of the particles, the sealing jaws must be kept open at least for the mean of $R(t_{res})$ plus a certain buffer time. In each cycle, if one or more particles are delayed more than that buffer time, there is a risk of the particle getting caught by the sealing jaws, which is often detrimental to the quality of the seam. Choosing overly long buffer times however, increases cycle time and therefore reduces bag output. In order to achieve optimal profitability, it is therefore crucial to accurately estimate the residence time range $R(t_{res})$ and its variation between cycles.

The falling behavior of the bulk material largely depends on the kinetics of contacts between particle-particle and particle-wall contacts [3]. Furthermore, the particles experi-

ence air resistance during the fall. Frank et al. showed that the vertical filling process can be described numerically with the Discrete Element Method (DEM) [4]. However, their model did not consider air resistance and required a separate test for model calibration. Kirsch showed that model calibration can be performed in the filling process itself but he also did not include air resistance. [1]

Coupling the DEM with computational fluid dynamics (CFD) is a widely used technique to account for the interaction between fluid and particles [5]. However, sophisticated CFD methods significantly increase computational cost compared to the DEM alone [6]. The aim of this study was to evaluate, if a much simpler formulation for drag can improve the DEM model enough to accurately describe the filling process. For this purpose, experiments and simulations were conducted for two different granular foods. Firstly, we obtained parameters from bulk calibration according to the state of the art, using a funnel discharge test, where the air influence was assumed to be negligible. The obtained parameters were validated in three different scenarios of a vertical drop, which revealed notable deviation from the experimental references, especially for the good with lower particle density.

In order to improve the physical accuracy of the model, a simple relation for air drag was introduced characterizing the free fall of a single particle. While this method fails to capture swarm effects, it is computationally cheap. In order to account for the slipstream effect of particles behind the bulk front, the drag correlation was turned off after the bulk front left the bottom of the tube. The model validation was repeated with he air drag model. While with high solid density, the simulations showed good agreement with the experimental references, the prediction was poorer for lower solid density. Finally, the calibration was repeated in the drop process itself (in-situ calibration) with the drag model. The predictions from the re-calibrated models are in good agreement with the experiment with a maximum of 5% deviation of the average and median of $R(t_{res})$. This indicates the validity of the chosen drag model for the presented cases, despite its simplicity.

2 DISCRETE ELEMENT SIMULATION

2.1 Contact formulation

Granular dynamics are largely determined by contacts between the particles. Particle contacts cause fairly complex elastic and plastic deformations, which are impractical to describe in full detail if a large quantity of particles is to be included in a simulation. The Discrete Element Method simplifies contacts to save numerical cost. Since the deformations are often much smaller than the particles' dimensions, they are neglected with regard to particle shape. The particles are thus considered as rigid bodies, often spheres. However, the particles are allowed to overlap upon contact. The normal and tangential forces resulting from contact are then described by empirical relations between overlap and force magnitude and direction. For the present study, the elastic-plastic linear hysteresis model was used [8], which follows Hooke's spring law but uses a higher spring constant for the relaxation after contact, to account for the energy dissipation due to plastic deformation.

2.2 Contact parameter identification

DEM simulations require a series of contact parameters, such as friction and restitution coefficients. These parameters are difficult to determine experimentally, since no standard tests are available. Furthermore, due to the empirical nature of the DEM contact laws, the physically accurate parameters may fail to compensate model errors, which often makes it necessary to use nonphysical "effective" parameter values. [9, 10] In practice, the contact parameters are thus often not measured but "calibrated" by iteratively tuning their values so that the DEM simulation reproduces a certain outcome of an experiment with the bulk good [7, 9, 11, 12, 10].

For model calibration, most studies rely on a dedicated lab-scale calibration test, which allows quick tests and is usually simpler to reproduce in the simulation than the actual process. However, only parameters that play a significant role in determining the calibration trials outcome can be determined this way [13]. The actual process however might be sensitive to additional parameters. A way to achieve identical parameter sensitivity in the calibration test and the actual process, is to perform the calibration in-situ, i.e. in the process of interest itself. Kirsch compared in-situ calibration in the drop process to calibration in a separate trial and showed both methods provided good model fidelity [1].

2.3 Effects of model shortcomings

Model calibration is an example for inverse approach and as such is sensitive to incomplete physics in the simulations [14]. In the case of vertical filling, DEM-only simulations neglect the influence of air drag on the particles. If the influence of drag is significant, this will introduce a bias to the solver. The parameter set with the lowest error is then only apparently optimal, and will, to some degree, differ from the actual optimal parameter set. Thus, the question is, if the influence of air significantly affects the falling behavior of the bulk. It has been shown that the speed of particle clusters falling in a vertical tube exceed the terminal velocity of a single particle [15]. This is an indication that a clustered drop resembles more a fall in vacuum. However the authors stated, that this is only to be assumed for drops with a low void fraction.

3 PARAMETER IDENTIFICATION

3.1 Experimental setups

The experiments were performed with two sample goods: near spherical bite-size chocolate candy and puffed rice. Their dimensions, bulk densities and sample masses used are noted in table 1.

Two different experimental setups were used in this study: a funnel discharge test with a dense particle flow [1] and a dilute drop test mimicking the industrial filling process [16]. The funnel setup was constructed from transparent polycarbonate. This allowed tracking the bulk's motion over time upon release. The experiments were filmed with a high speed camera at 100 frames/second. The videos were processed with the Matlab® Image Processing Toolbox™, so that the visible area of particles was extracted (figure 2). The experiments were each repeated five times and the resulting time signals were

Table 1: Set bulk good parameters.

Material	Parameter	Value	Sample masses
Chocolate Candy	Young's Modulus	10^7 m	
	Bulk density	662 kg/m^3	2000 g$^{\nabla}$, 300 g, 500 g, 700 g*
	Particle diameter d	11.2 mm	
Puffed Rice	Young's Modulus	10^7 m	
	Bulk density	129 kg/m^3	230 g$^{\nabla}$, 50 g*, 100 g, 200 g
	Particle diameter d	4.8 mm	
	Particle length l	9.0 mm	
Polycarbonate	Young's Modulus	10^7 m	–

$^{\nabla}$ Funnel discharge calibration
* Drop test calibration

averaged.

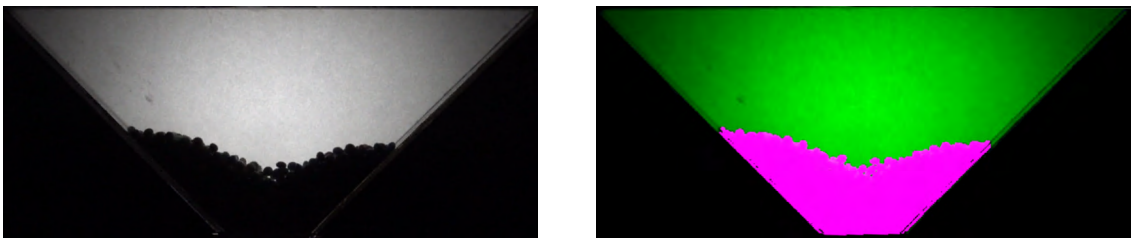

(a) Original frame. (b) Result of binarization.

Figure 2: Experimental funnel discharge test and image processing to obtain visible particle surface.

The drop test setup is shown schematically in figure 3a. Before each experiment, the sample bulk was placed in the sample bucket. The drop was then initiated by opening the motor-driven flaps. The drop experiments were filmed with a high-speed camera at 1024 frames/second. The videos were then processed using the Matlab® Image Processing Toolbox™ similar to the funnel test, so that the 2-dimensiona particle area could be extracted (figure 3b). This allowed calculating and tracking the virtual center of mass of the 2-dimensional projection over time [2]. Additionally, the time stamps t_{ftl} and t_{ltl} of the first and last particle to leave the tube at the bottom were extracted. Each test was conducted at least seven times and the resulting curves and the time stamps were averaged.

The experimental setup and the operation conditions were transferred into the DEM environment Rocky DEM. From every simulation run, a video mimicking the experimental videos was exported and analyzed analogously.

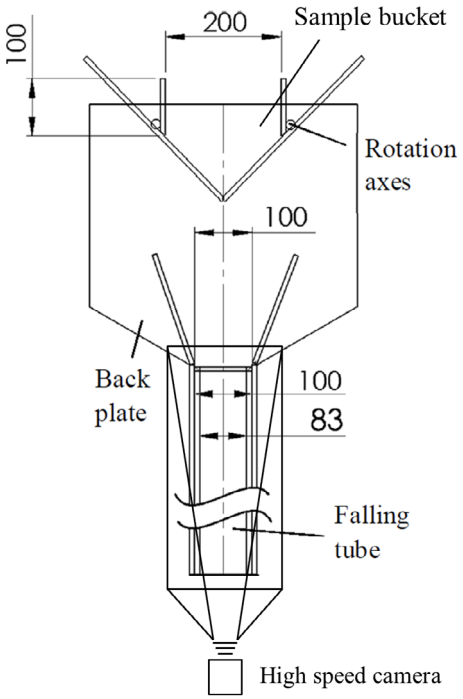

(a) Drop setup, measures in mm. The bulk sample can be released with motor-driven flaps. Adapted from [16].

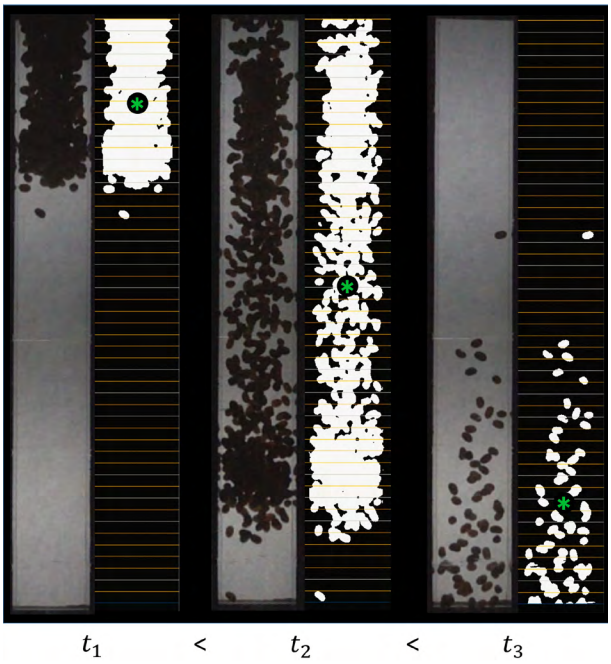

(b) Original and processed example video frames of the drop process. The asterisk shows the location of the 2D center of mass. From [2].

Figure 3: Experimental drop setup and image processing.

3.2 Parameter variation and regression of solver response

The aim of the calibration is to find the parameter set $\vec{x}_{opt}$ where the error between simulation and experimental reference becomes minimal. The error function $E(\vec{x})$ varied between calibration scenarios (see 3.3). Iterative calibration is numerically expensive, since every parameter combination tested requires one solver run. The development of efficient and reliable calibration procedure has gained the attention of several groups [1, 17, 13, 18]. Rackl et al. and Kirsch performed the calibration on a meta model, which was constructed from the responses of a predetermined number of solver calls at different parameter sets which were obtained from Latin Hypercube sampling (LHC) [1, 13, 19, 20]. The benefit of the meta model is, that it is much cheaper to evaluate than the DEM solver and thus allows for faster search of an optimal parameter set. Additionally, the regression is capable of smoothing out some random variation (solver noise), which makes optimization more efficient [21].

The parameter variation and optimization scheme is shown in figure 4 [1]. It was implemented using the optimization software package Optislang®. The scheme features an iterative adaptive approach where samples are added in the regions where the error function is low, to increase local resolution. Optislang® offers a measure for the fidelity

of the regression in the coefficient of prognosis [22]. The process was stopped if the coefficient of prognosis did not further increase. In all cases, a minimum of six iterations were performed. After the last sampling iteration, the parameter set with the lowest error between simulation and reference was identified. The resulting parameter set $\vec{x}_{opt}$ was then used for validation.

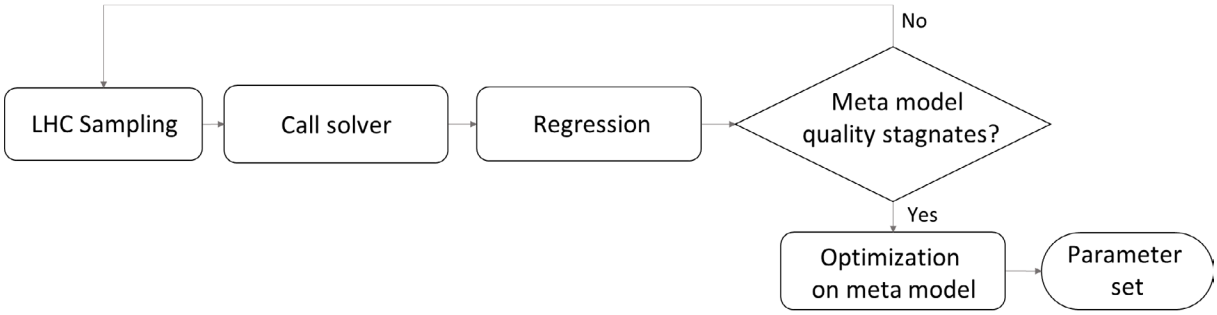

Figure 4: Workflow for DEM input contact parameter calibration (Adapted from [1]).

3.3 Calibration scenarios

The scheme described in section 3.2 was performed for two calibration scenarios and for both sample goods. The first scenario was the funnel discharge test as described above. The error function $E(\vec{x})$ was defined as the averaged absolute point-wise deviation between reference and simulation. Secondly, the drop test as described above was used for calibration. The error function $E(\vec{x})$ was the root mean square error (RMSE) of the virtual center of mass in longitudinal direction between reference and simulation [2]. For the second calibration, a CFD model was used to account for air drag.

Accurate descriptions of air resistance, for example FEM methods, describe the element-wise interaction between particles and the surrounding medium. This makes calculations significantly more expensive and would lead to impractical run times for model calibration. In order to avoid this issue, a much simpler approach for air drag was attempted for this study. It was reasoned that due to the dilute nature of the drop process, the air drag could be approximated by the case of a single particle falling through an unconstrained fluid domain (free fall). The drag force F_D in this case follows the relationship

$$F_D = \frac{1}{2}\rho v^2 C_D A_p \tag{2}$$

where ρ is the particle density, v the particle's velocity, and A_p it's cross sectional area. The drag coefficient C_D depends on the particle shape and on the Reynold's number. Many empirical relations for C_D can be found in literature. A commonly used relation for C_D based on the original formulation of Schiller and Naumann is given by [23, 24]:

$$C_D = max\left[\frac{24}{Re}\left(1 + 0.15Re^{0.687}\right), 0.44\right] \tag{3}$$

With this simple relationship for air drag, the effect of particle velocity is incorporated in the model, while the local particle concentration and the history of air displacement by leading particles is neglected. The latter slipstream effect results in particles behind the leading front to experience less air drag. In order to include this into the model, the air drag model was only used in the first half of every simulation until the particle front left the tube at the bottom. After this, the drag model was switched off, assuming a fall in vacuum. Due to the simplicity of the model, the air drag introduced should not be viewed as an expansion of the physics model, but rather as an empirical correction factor for the DEM simulations. Such an approach is only considered viable, as long as the influence of air drag is overall low compared to the influence of the particle contacts, which was first to be tested on the DEM models calibrated to the funnel experiment.

4 RESULTS AND DISCUSSION

4.1 Calibration to funnel test

The predictions of the DEM models calibrated to the funnel discharge test are shown in a box plot in figure 5. On the ordinate, the mass of the bulk sample and the source of the data are given (experimental reference, simulation in vacuum or simulation with CFD). The vertical line in the box plot marks the median and the box edges indicate the first and third quartile. The whiskers indicate the most extreme observations that still fall within 1.5 times the interquartile range. All other observations are marked with a plus sign and indicate outliers.

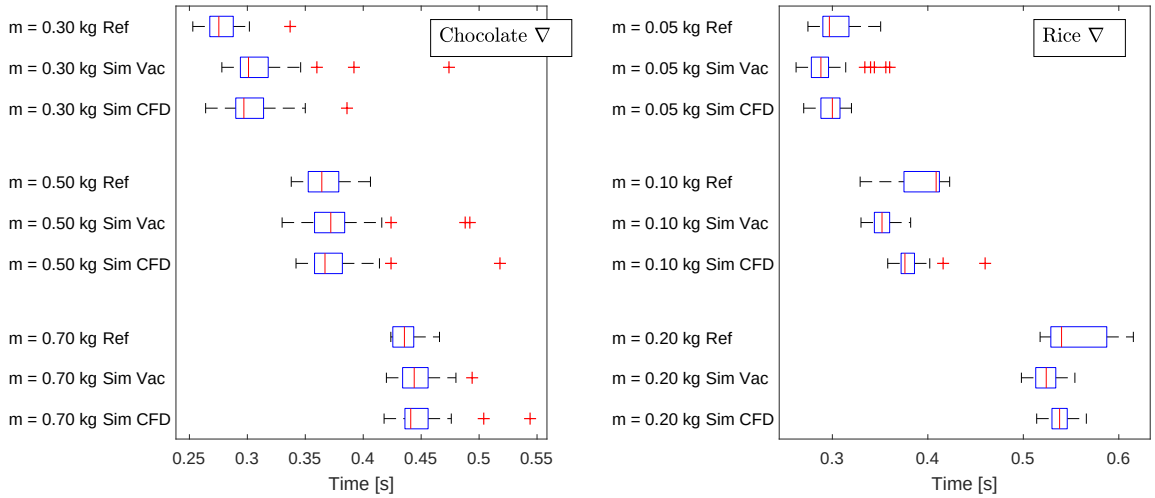

(a) Residence time range $R(t_{res})$ of chocolate candy.

(b) Residence time range $R(t_{res})$ of puffed rice.

Figure 5: Validation of the models calibrated in the funnel discharge test.

We find a notable deviation between the experimental data and the simulations, which varies from case to case. Furthermore, we find that the drag model has little impact for the

chocolate candy, but notably influences the simulations with puffed rice. In the latter, the drag model improves the prediction of the simulation, by reducing the underestimation of the residence time range. These results give an indication that the chosen CFD model is a viable correction factor for air drag.

4.2 Calibration to drop test with drag model

Based on the previous findings, a new set of two calibration runs with the drag model was performed in the drop test with the bulk masses indicated in table 1. The results of the validation of the calibrated models are shown in figure 6.

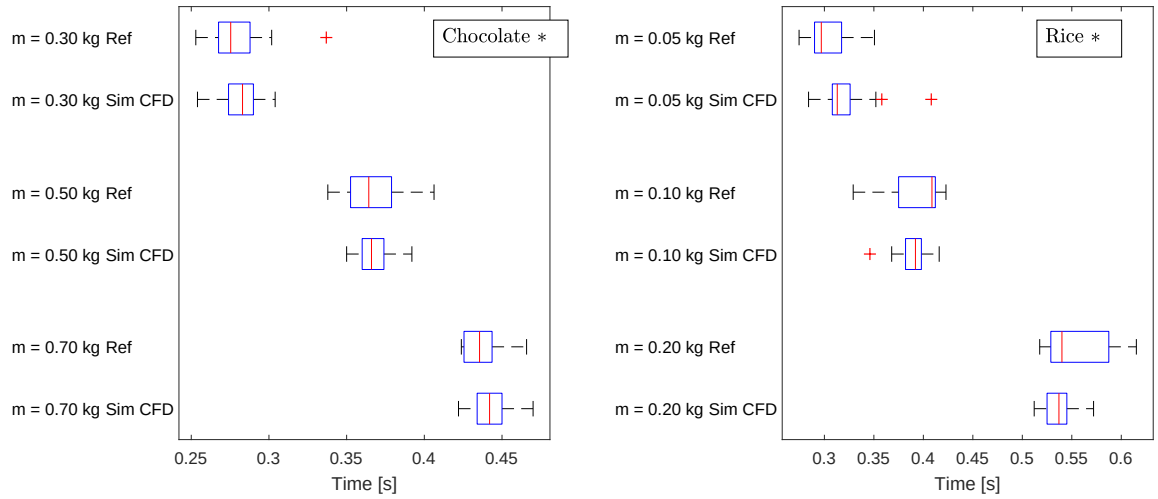

(a) Residence time range $R(t_{res})$ of chocolate candy.

(b) Residence time range $R(t_{res})$ of Puffed rice.

Figure 6: Validation of the models calibrated in the drop test with CFD model.

For the chocolate candy, we find a better agreement between reference and simulation (figure 6a) than in the validation of the model calibrated to the funnel test before. (figure 5a). More specifically, the prediction of the median is more accurate and more consistent over the sample mass. Secondly, the location and distance of the first and third quartile show a much better agreement between reference and simulation than in figure 5a. This is an indication, that the model could also be used to make statistical predictions. This would be of especially high importance for industry application, since the filling process is intrinsically random. Thus, if a model is capable of predicting "worst cases", i.e. abnormally long $R(t_{res})$, and their likelihood, one could infer economically beneficial settings of the filling process, considering earnings for bags output versus cost for possible machine downtime when a particle was caught between the sealing jaws.

For the DEM-CFD for puffed rice (figure 6b), we find a comparable prediction accuracy as in the model calibrated to the funnel test (figure 5b). We find notable deviation in the median of a maximum up to 5% for the cases with lower sample mass, which could

still be considered acceptable for practical use. The predictions for statistical spread now also show notable deviation. This would make the model for puffed rice less reliable for predictions in an industrial context. A reason for the deviation is that the impact of air resistance seems to be larger than for the chocolate candy (figure 5). This is explainable by the lower density of the puffed rice particles, which could mean that the real air flow plays a larger role. Thus, these simulations might require a more sophisticated drag model.

5 CONCLUSION

The aim of this study was to find a computationally cheap CFD model, capable of correcting the DEM model's shortcomings regarding air drag for the simulation of the industrial vertical filling process. We showed in a simplified drop setup that a fairly simple relationship for air drag was capable of providing a plausible correction to DEM models so that their predictive capability was improved. Furthermore, the CFD model was implemented in an in-situ calibration approach, meaning that the DEM parameters were calibrated in the process of interest itself. The calibrated models show good agreement with the median observation from the measurements and even predict the statistical spread fairly reliably for denser particles. Both are important for industrially relevant choices regarding machine operation.

ACKNOWLEDGMENTS

The author would like to thank Robert Bosch Packaging Technology B.V. for funding this research project. Further tanks go to the department for engineering and development and the members of TU Dresden's chair of Processing Machines and Processing Technology for their support and feedback. Lastly, thanks goes to the head of the chair for the academic supervision of the project.

REFERENCES

[1] Kirsch, S. DEM model calibration for vertical filling: Selection of adequate trials and handling randomness. *Weimar Optimization and Stochastic Days* (2018).

[2] Kirsch, S. Stochastic discrete element modelling of granular filling processes for industry application: Can we formulate a standardized approach? *7th International Computational Modelling Symposium* (2019).

[3] Pöschel, T and Schwager, T. *Computational Granular Dynamics: Models and Algorithms*. Springer-Verlag Berlin Heidelberg, (2005).

[4] Frank, M. and Holzweißig, J. Simulation-based optimization of geometry and motion of a vertical tubular bag machine. *Research report, Sächsische Landesbibliothek.* (2016).

[5] Zhu, H.P., Zhou, Z.Y., Yang, R.Y. and Yu, A.B. Discrete particle simulation of particulate systems: A review of major applications and findings. *Chem. Eng. Science* (2008) **63**(23):5728–5770.

[6] Zhu, H.P., Zhou, Z.Y., Yang, R.Y. and Yu, A.B. Discrete particle simulation of particulate systems: Theoretical developments. *Chem. Eng. Science.* (2007) **62**(13):3378–3396.

[7] Markauskas, D. and Kacianauskas, R. Investigation of rice grain flow by multi-sphere particle model with rolling resistance. *Granular Matter* (2010) **13**(2):143–148.

[8] Luding, S. Collisions and contacts between two particles. *Physics of Dry Granular Media* **350**:285–304.

[9] Coetzee, C. J. Review: Calibration of the discrete element method. *Powder Technol.* (2017) **310**:104–142.

[10] Barrios, G.K.P., de Carvalho, R.M. and Kwade, A. and Tavares, L.M. Contact parameter estimation for DEM simulation of iron ore pellet handling. *Powder Technol.* (2013) **248**:84–93.

[11] Roessler, T. and Katterfeld, A. DEM parameter calibration of cohesive bulk materials using a simple angle of repose test. *Particuology* (2018) **343**:803—812.

[12] Coetzee, C. J. Calibration of the discrete element method and the effect of particle shape. *Powder Technol.* (2016) **297**:50–70.

[13] Rackl, M. and Hanley, K.J. A methodical calibration procedure for discrete element models. *Powder Technol.* (2017) **307**:73–83.

[14] Pernot, P. and Cailliez, F. A critical review of statistical calibration/prediction models handling data inconsistency and model inadequacy. *Transport Phenomena and Fluid Mechanics* (2017) **63**.

[15] Nakashima, K., Johno, Y. and Shigematsu, T. Free fall characteristics of particle clusters in a vertical pipe. *Journal of Physics: Conference Series* (2009) **147**(1).

[16] Kirsch, S. and Philipp, A. Simulation of vertical filling processes of granular foods for typical retail amounts. *9th Conference Processing Machines and Packaging Technology Dresden* (2018).

[17] Benvenuti L., Kloss C. and Pirkera S. Identification of DEM simulation parameters by artificial neural networks and bulk experiments. *Powder Technol.* (2016) **291**:456–465.

[18] Roessler, T., Richter, C., Katterfeld, A. and Will, F. Development of a standard calibration procedure for the DEM parameters of cohesionless bulk materials – part I: Solving the problem of ambiguous parameter combinations. *Powder Technol.* (2018) (343):803–812.

[19] McKay, M. D., Beckman, R. J. and Conover and W. J. A comparison of three methods for selecting values of input variables in the analysis of output from a computer code. *Technometrics* (1979) **21**(2):239–245.

[20] Helton, J.C. and Davis, F.J. Latin hypercube sampling and the propagation of uncertainty in analyses of complex systems. *Reliab. Eng. Syst. Safe.* (2003) **81**:23–69.

[21] Barton, R.R. and Meckesheimer, M. Metamodel-based simulation optimization. *Handbooks in Operations Research and Management Science* (13):535–574 Elsevier (2006).

[22] Most, T. and Will J. Metamodel of optimal prognosis - an automatic approach for variable reduction and optimal metamodel selection. *Weimar Optimization and Stochastic Days* (2008).

[23] Schiller, L. and Naumann A. A drag coefficient correlation. *Zeitschrift des Vereins Deutscher Ingenieure* (1935) (77):318–320.

[24] *Fluent Theory Guide* ANSYS, Inc., (2013).